Forensic Science International 228 (2013) 75–82

Contents lists available at SciVerse ScienceDirect

Forensic Science International

journal homepage: www.elsevier.com/locate/forsciint

Blood drop size in passive dripping from weapons

N. Kabaliuk [a], M.C. Jermy [a,*], K. Morison [b], T. Stotesbury [c,d], M.C. Taylor [d], E. Williams [c,d]

[a] Department of Mechanical Engineering, University of Canterbury, Private Bag 4800, Christchurch 8041, New Zealand
[b] Department of Chemical and Process Engineering, University of Canterbury, Private Bag 4800, Christchurch 8041, New Zealand
[c] Forensic Science, School of Chemical Sciences, University of Auckland, Private Bag 92019, Auckland 1142, New Zealand
[d] Christchurch Science Centre, Institute of Environmental Science and Research, 27 Creyke Road, Christchurch 8041, New Zealand

ARTICLE INFO

Article history:
Received 21 August 2012
Received in revised form 10 February 2013
Accepted 12 February 2013
Available online

Keywords:
Bloodstain pattern analysis
Dripping
Drop size
Accompanying drop
Blood
Spatter

ABSTRACT

Passive dripping, the slow dripping of blood under gravity, is responsible for some bloodstains found at crime scenes, particularly drip trails left by a person moving through the scene. Previous work by other authors has established relationships, under ideal conditions, between the size of the stain, the number of spines and satellite stains, the roughness of the surface, the size of the blood droplet and the height from which it falls. To apply these relationships to infer the height of fall requires independent knowledge of the size of the droplet. This work aims to measure the size of droplets falling from objects representative of hand-held weapons. Pig blood was used, with density, surface tension and viscosity controlled to fall within the normal range for human blood. Distilled water was also tested as a reference. Drips were formed from stainless steel objects with different roughnesses including cylinders of diameter between 10 and 100 mm, and flat plates. Small radius objects including a knife and a wrench were also tested. High speed images of the falling drops were captured. The primary blood drop size ranged from 4.15 ± 0.11 mm up to 6.15 ± 0.15 mm (depending on the object), with the smaller values from sharper objects. The primary drop size correlated only weakly with surface roughness, over the roughness range studied. The number of accompanying droplets increased with the object size, but no significant correlation with surface texture was observed. Dripping of blood produced slightly smaller drops, with more accompanying droplets, than dripping water.

1. Introduction

Bloodstain patterns at scenes of violent crime are often analyzed in an attempt to reach conclusions about the events that gave rise to these patterns. Determining the location and nature of the blood source at the time the bloodstain pattern was formed is often of relevance when drawing these conclusions. Central to any inference about the blood source is an estimation of blood drop volume and velocity.

For passive drops, formed as a result of dripping of blood from a wound or bloodied object under the action of gravity only, it is recognized that the volume of a drop depends on characteristics of the object from which it originates (such as its geometry, surface texture and wettability) [1–3] and on the dripping liquid properties and flow rate [4,5]. Parker et al. [4] reported the range of drop volumes from 42 μL (eye dropper) to 87 μL (pre-wetted palm of the hand). The drop volumes were determined by collecting and measuring the volume of a known number of drops, and so tend to be overestimates when small satellite or accompanying droplets are present. Ross [5] looked at a range of objects that could be used as weapons and showed that drop volumes varied from 30 μL (small kitchen knife) to 210 μL (hammer). She also used a volumetric method and noted the presence of what she termed "follow-on" drops. The results, in addition, were influenced by the varying flow rate of dripping from weapons dipped into blood.

There have been several attempts to correlate blood stain size and shape to the volume and velocity of a passive drop [6–10]. In particular, Balthazard et al. [6] focused on the relationship between the stain size and drop velocity, whereas MacDonnell and de Lige [7] sought to develop a relationship that would enable the volume of a blood drop to be estimated from a bloodstain of known size. Knock and Davidson [8] and Hulse-Smith et al. [9,10], in turn, showed that under well-controlled conditions it is possible to determine both volume and velocity of a drop from the diameter of the stain and the number of spines on the stain margin. This method, however, has several limitations such as the reproducibility in the counting of spines and the limited number, or even absence, of spines for low velocity impact on some surfaces.

A number of theoretical attempts were made to estimate the volume of a drop produced as a result of dripping of a liquid other than blood from a surface or orifice. The theory describing the

* Corresponding author.
E-mail address: mark.jermy@canterbury.ac.nz (M.C. Jermy).

0379-0738/$ – see front matter © 2013 Elsevier Ireland Ltd. All rights reserved.
http://dx.doi.org/10.1016/j.forsciint.2013.02.023

equilibrium shape of a hanging volume of liquid is described by Fordham [11] and Stauffer [12]. Tanasawa and Toyoda [13] analyzed the dripping of a liquid film on the underside of a flat plate and calculated the slow development of the pendant drop up to the first breakup.

The dynamics of a liquid ligament and conditions for its breakup of were also studied both experimentally and numerically for fluids other then blood for low dripping flow rates [14–18].

Lefebvre [19] reported an equation (Eq. (1)) for the size of a drop falling from the underside of a flat plate, and references Lapple et al. [20], who in turn reference Tamada and Shibaoka [21]. However this equation does not appear in Tamada and Shibaoka's paper [21] or Hida and Nakanishi's paper [22] and may be a correlation to their data.

$$d_{\text{drop}} = 3.3\sqrt{\frac{\sigma}{\rho g}} \tag{1}$$

In Eq. (1), d_{drop} is the diameter of the drop, σ is the surface tension of the liquid, ρ the density of the liquid and g the acceleration due to gravity.

In this light, an alternative method to determine the range of the variability of passive blood drop volumes excluding the contribution of smaller satellite droplets as well as a study of the influence of the dripping surface characteristics on the process of drop formation (and so on the resulting drop volume) would complement previous studies.

The purpose of the present work is therefore to reconsider the relationship between the volume of a drop formed by passive dripping and geometry and surface texture of a dripping object providing the constancy of its surface properties (or resistance to corrosion and staining) as well as dripping liquid temperature, flow rate and composition. To this end, dripping experiments with non-absorbent metallic surfaces representative of weapons frequently used in criminal assaults were conducted. High speed imaging was used to directly measure the size of the primary drop, distinct from the accompanying droplets, and count the number of the later.

2. Methodology

2.1. Test objects

Liquid drops were allowed to form from the surface of a number of objects representing common weapons (Fig. 1 and Table 1). Among them were five sets of AISI 304 stainless steel cylinders of diameter between 10 and 100 mm and two flat plates with different surface roughness.

Different surface textures were produced by turning the cylindrical samples on a lathe and by vertical milling the flat samples. As a result the machining marks of the cylinders followed the circumferential direction (perpendicular to their axis of symmetry) whereas the flat plates had cross-hatched patterns.

It should be noted that each machining process removed a small amount of material from the specimen's surface to produce a higher degree of surface finish. Rougher surface finishes required more machining, so the actual diameter for the cylindrical objects tended to decrease slightly as the roughness increased.

A Taylor-Hobson TALYSURF 10 profilometer was used to measure average roughness values, $R_a = \bar{R}_i$ (Fig. 2). R_i is half the average vertical difference between a peak and the adjacent valley. The profilometer tip was run in a direction perpendicular to the surface texture direction. Eight tests were performed with each object. The waviness (long wavelength undulation) of the machined surface profile was considered to be small and was not investigated.

Table 1
Dimensional and surface characteristics of the objects tested.

Object description	Surface characteristic			
	H (mm^{-1})	R_a (μm)		
		'Smooth'	'Medium'	'Rough'
Cylinders	0.010	0.19 ± 0.02	3.59 ± 0.16	~12.5
	0.013	0.13 ± 0.09	2.4 ± 0.1	~12.5
	0.025	0.17 ± 0.02	~6.3	~12.5
	0.050	0.55 ± 0.19	3.7 ± 0.17	~12.5
	0.10	0.66 ± 0.07	~6.3	~12.5
Flat plates	~0	0.37 ± 0.05	~6.3	–
Wrench	~0.20		–	
Knife	~5.25		–	

Surface roughness values of the 'medium' cylindrical samples (10.01 mm and 39.5 mm in diameter) and all 'rough' samples were visually and tactile assessed using surface roughness standards, comparator Flexbar composite set no. 16008.

The samples were then grouped in three categories: smooth with 0.1 μm < R_a < 0.7 μm, medium with 2.4 μm < R_a < 6.3 μm and rough objects with R_a ~12.5 μm.

Experimental data was assessed in terms of the mean curvature H of the test object surface as a measure of its convolution or deviation from flatness:

$$H = \frac{1}{2}\left(\frac{1}{R_1} + \frac{1}{R_2}\right),$$

where R_1 and R_2 are the principal radii of curvature, or maximum and minimum perpendicular radii of the surface curvature of the object from which the drops are formed. These are measured at a point on the surface in perpendicular (or principal) directions.

Flat surface objects had radii of curvature which tend to infinity and hence had close to zero mean surface curvatures. Each cylindrical test object had one radius of curvature equivalent to its geometrical radius and an infinite radius of curvature corresponding to its axial length. Mean surface curvature for these samples ranged from about 0.1 to 0.01 mm^{-1}.

A stainless steel kitchen knife and a chrome vanadium metric wrench were also tested. The knife blade had a body with flat parallel surfaces and an edge with a radius of curvature of about 20 cm. The point of the knife had a radius of curvature of a few millimeters in the plane of the blade and a fraction of a millimeter in the other direction (see Fig. 3) which gave H of about 5.25 mm^{-1}.

The wrench open end (opposite to the ring end) had a radius of curvature of a few centimeters in one direction, and a few millimeters in the other corresponding to H of about 0.2 mm^{-1}.

Smooth and rough cylinders were 50 mm long. The length of the medium-roughness samples was 100 mm. The flat plates were 100 mm × 100 mm × 5 mm in size. The uncertainty in the dimensional measurements was ±0.02 mm. The absolute errors in the measured roughness values in Table 1 include both the profilometer instrumental uncertainty and the standard deviations of the mean values for a 95% confidence interval.

Before each test all objects were carefully cleaned with 1% Virkon solution, rinsed with distilled water, acetone and ethanol and then dried in hot air to remove any deposits on their surfaces.

Fig. 1. Objects tested.

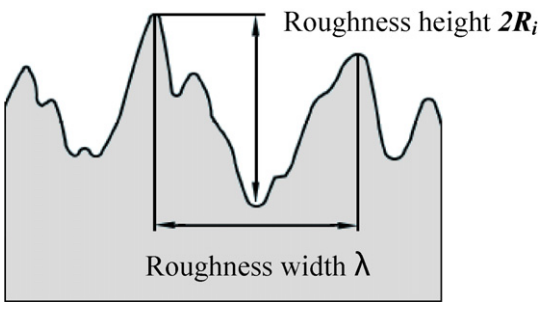

Fig. 2. Basic surface texture characteristics.

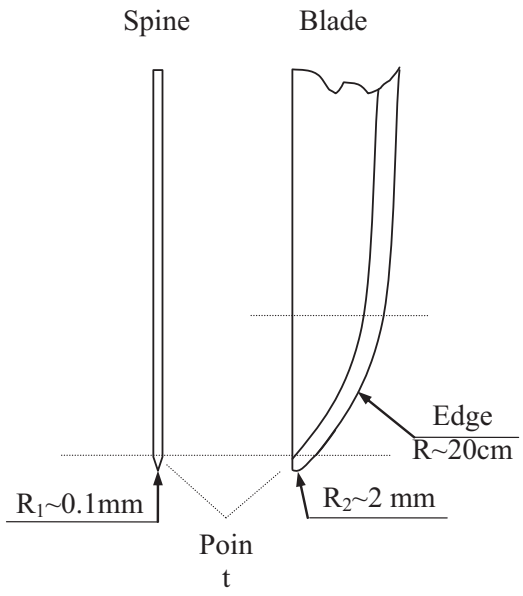

Fig. 3. Knife diagram.

2.2. Test liquids

Both distilled water and 1-day-old abattoir porcine blood, used as a human blood substitute, were tested. Porcine and human blood have been shown to have similar physical properties and produce droplets similar in size [23]. To prevent the blood from clotting, EDTA was added at a concentration of 7 mg/mL of blood. The blood was stored at 4 °C for 24 h before experimentation.

Density, surface tension and viscosity of porcine blood were controlled to match human values before and after the experiments. Measured mean values of blood density, surface tension and viscosity together with the additional measurements of blood packed cell volume (PCV) and plasma viscosity are listed in Table 2. Before each physical property measurement, calibrations with distilled water were conducted. The table includes data from distilled water calibrations and calculated absolute errors. Density and surface tension tests were performed with the blood warmed to 37 ± 0.5 °C in a water bath.

Temperature measurements for this study were obtained using Yokogawa TX10 digital thermometer.

The density of porcine blood was measured by a weighing syringe method using a Sartorius analytical balance ED224S. Six independent measurements were taken and averaged. Corrections of the order of 1% were applied, based on the calibration with distilled water.

Surface tension measurements were performed on a KSV Contact Angle and Surface Tension Meter with a CAM 200 CCD camera and CAM 2008 software. A 1.25 mm diameter hypodermic needle and a syringe were used to produce fifteen pendant blood drops with fully developed (elongated) neck. Before each test the needle was cleaned with 1% Virkon solution, rinsed with distilled water and acetone, then carefully dried with a hot air gun. Droplet images were captured and analyzed by fitting a curve to the image profile. The mean surface tension and standard deviation of the mean were calculated.

Packed cell volume (PCV) of pig blood was measured after 4 min centrifugation at 12,000 rpm in a Hettich EBA 21 Centrifuge (Andreas Hettich CmbH & Co. KG). An average value was taken from six capillary tube readings. Only slight, if any, haemolysis was visually observed in blood which had been used in the dripping experiment.

Porcine whole blood and plasma viscosity were measured at a shear rate of $1000\ s^{-1}$ with a rotational rheometer HAAKE Rotovisco RV 20 with NV coaxial cylinders sensor system. The rheometer heating bath thermocontroller HAAKE F3 maintained blood at 37 ± 0.01 °C. Two verification runs were made for each sample. Shear stress correction factors of the order of 3% and instrumental error based on the device calibration with a general purpose viscosity reference standard type N10 (Paragon Scientific Ltd.) were applied to the obtained data.

2.3. Drop formation

Liquid was introduced at the top of the object and allowed to flow over the surface to the lowest point, where the drops formed. A peristaltic pump (Gilson Minipuls 3 M312, Gilson LTD) with a speed controller and 4 mm diameter silicone tubing was used to draw the liquid from a reservoir flask to the experiment. A constant flow rate of 0.1 ± 0.02 mL/s (measured by weighing) was maintained. Distilled water was tested at ambient temperature 22 ± 0.5 °C. The blood was heated to 37.5 ± 0.5 °C in a reservoir flask placed in the water bath, both agitated by magnetic stirrers. The temperature of the blood leaving the supply tube was 36.8 ± 0.5 °C, but the objects were at ambient temperature 22 ± 0.5 °C.

For each object studied and for each liquid tested, the formation process of twelve drops was captured on a Redlake MotionPro v3 (CCD or CMOS, resolution 1280×1024 pixels) at 1040 frames per second. Motion Studio Ver. 2.09.00 (Integrated Design Tools (IDT), Inc.) software was used to operate the camera. The experimental set up was side- and back-lit by 0.5–2 kW incandescent lamps placed behind diffusing screens of sandblasted PMMA. The images were processed with Photron FASTCAM Viewer Ver.3.0 (Photron Ltd.) software.

Horizontal and vertical diameters of the primary drop were measured as it passed through the approximately spherical phase of its oscillation and then averaged. A distance calibration (pixels/mm) was made using an image of a steel ruler. Typical magnifications of 14 pixels/mm were used. The ruler was mounted vertically as close as possible to the object plane of the camera and within ±2 mm of the perimeter of drop formation on the object surface. The second parameter of interest was the number of accompanying (satellite) droplets produced from the ligament breakup. Accompanying droplets were allowed to fall 6 cm from the object surface to ensure the cessation of inter-droplet interactions (collision and coalescence [36]) and were then counted. Absolute uncertainties based on the standard deviation of the mean and instrumental uncertainties for each set of the experiments were calculated for a 95% confidence interval.

The dripping rate of test liquids, i.e. the number of drops detached from the object in unit time was assessed by measuring the time for 10 drops to detach using a digital stopwatch. The relative error of these indirect measurements was less than 3%.

3. Results

The primary drop size and number of accompanying droplets formed from objects of different surface curvature and roughness are shown in Figs. 4 and 5. The plots include data from dripping experiments with distilled water and with porcine blood, and error bars are equal to two times the square root of the sum of squares of the instrument error Δ_{in} (one pixel) plus the standard deviation of the mean $\bar{S}_n$ multiplied by Student's coefficient $t = 2.2$ for 12 measurements and a 95% confidence interval: $\Delta = \sqrt{(\Delta_{in})^2 + (t\bar{S}_n)^2}$,

The mean primary drop size, for both distilled water and blood, decreased as the object surface mean curvature increased over the

Table 2
Measured physical properties of porcine blood and distilled water. Errors listed are either sample standard deviations or absolute errors for a 95% confidence interval.

	Before the experiment	After the experiment	# of measurements	Published reference values
Pig blood				
Age since collection from a pig	1-Day-old	2-Days-old	–	
PCV	0.39 ± 0.01	0.388 ± 0.006	6	0.40–0.45 [24]
Density ($\times 10^3$ kg/m^3)	1.069 ± 0.022	1.069 ± 0.021	5	1.052–1.063 [25–27]
Surface tension (mN/m)	62.47 ± 0.71	62.96 ± 0.49	15	55.5–63.1 [28,29]
Whole blood viscosity at $1000\ s^{-1}$ (mN s/m^2)	4.001 ± 0.008	4.133 ± 0.008	2	3.2–4.4 [30–34]
Plasma viscosity (mN s/m^2)	1.482 ± 0.003	–	2	1.025–1.029 [30,31]
Distilled water				
Density at 22 °C ($\times 10^3$ kg/m^3)	1.007 ± 0.028	0.993 ± 0.030	5	0.998 [35]
Surface tension at 22 °C (mN/m)	71.87 ± 0.35	72.06 ± 0.37	15	72.75 [35]
Viscosity at 22 °C (mN s/m^2)	–	–	–	1.002 [35]

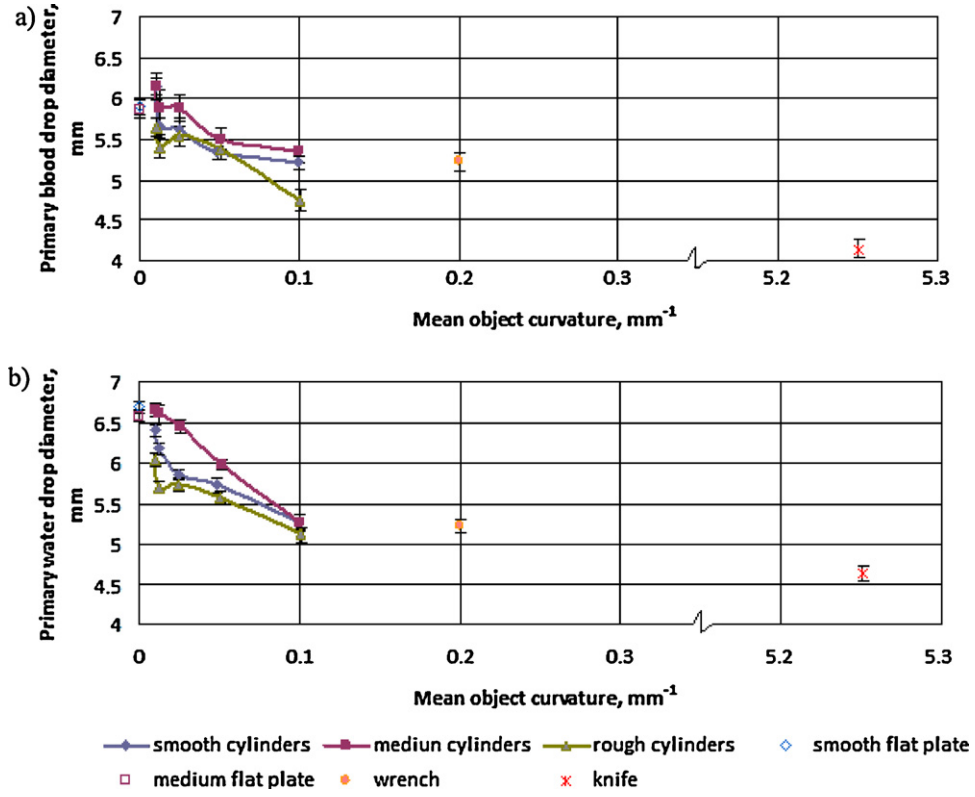

Fig. 4. Primary drop diameter for (a) porcine blood and (b) distilled water.

range of 0.1–5.25 mm^{-1} (sharper objects), but was relatively constant for the blunt objects tested.

The primary water drops tended to be slightly larger than blood drops. The observed range of blood drop diameters was 4.15 ± 0.10 mm (knife) to 6.15 ± 0.17 mm (cylinder with $H = 0.01$ mm^{-1} and 3.59 μm roughness). This corresponds to drop volumes of between 37.4 μL and 121.8 μL. Water drops varied in diameter from 4.63 ± 0.10 mm (knife) to 6.68 ± 0.05 mm (flat plate,

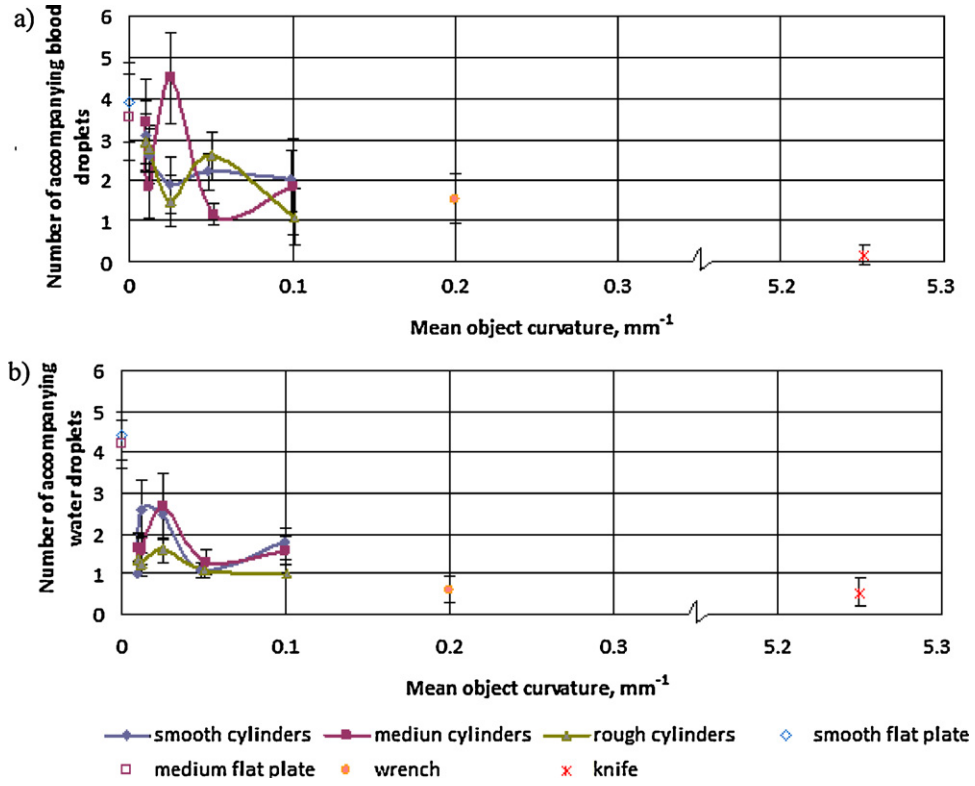

Fig. 5. Number of accompanying (a) porcine blood and (b) distilled water droplets formed from the studied objects.

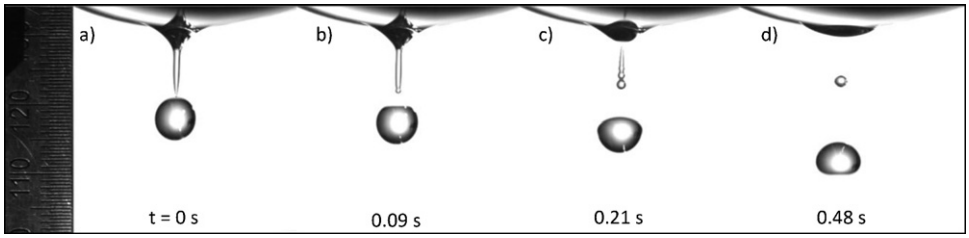

Fig. 6. Dripping of water from the cylindrical object with $H = 0.013\ mm^{-1}$ and 2.4 μm surface roughness. Smallest scale division is 0.5 mm.

0.37 μm rough). This corresponds to drop volumes of between 52.0 μL and 156.1 μL. Blood drops tended to be more variable in size than water drops for a given object.

For the cylinders, primary drop size correlated, although weakly, with object roughness over the roughness range studied, both for water and for blood. The correlation is weaker for blood than for water. The maximum observed deviation in mean drop diameter due to difference in roughness of a particular sample was 0.9 mm for blood and 0.6 mm for water.

However, the obtained data showed a slight increase in the mean primary drop size as the object's roughness increased from 0.4 μm (smooth samples) to 6.3 μm (medium samples). A further increase in roughness to about 12 μm led to a decrease in drop size. This was seen in both water and blood data. The flat plates show no change in primary drop size due to roughness.

The number of accompanying water and blood droplets decreased with the object surface curvature (from blunt to sharp weapons), but the trends were not clear because of the high variability in the data (Fig. 5(a) and (b)). No statistically significant correlation with the surface roughness was observed.

Blood was observed to produce a slightly higher number of accompanying droplets compared to water.

The dripping rate of blood was generally higher than that of water, though of the same order of magnitude. Dripping rate was observed to increase with the surface curvature of the object from which either blood or water was dripping within the range of about 0.5–0.6 for flat objects to 2–2.5 drops per second for the sharpest object tested, knife. 5–8% difference in the dripping rate was associated with the difference in the roughness of the wetted object with higher values for rough objects and lower for medium ones, compared to the smooth objects tested.

The process of passive blood drop formation differed from the formation of water drops and seemed to be more complex and variable. For both liquids, the process began with the slow formation and growth of a pendant drop at the lowest point of the object under the action of gravity. A drop with the critical weight then started to fall, but remained connected to the volume of liquid adhering to the object surface (residual liquid) by a liquid neck. The neck then elongated forming a thin ligament.

With water, uniform axisymmetric cylindrical ligaments were observed in all test cases. The water ligament when narrow enough broke up first at the bottom near the primary drop (Fig. 6(a)). The surface tension force at the ligament's highly curved lower end pulled it upward (Fig. 6(b)). Surface instabilities (waves) occurred, grew and propagated upward and eventually reached the upper end of the ligament. The ligament then broke off from the residual liquid at the top and contracted vertically into one or more accompanying (or satellite) droplets (Fig. 6(c) and (d)). These oscillated in shape and occasionally collided or bounced from each other and moved with different velocities and trajectories.

For the case of the dripping of blood, ligaments generally had non-uniform (stepped) shapes (though they are axis-symmetric). A number of liquid bulges (satellite beads) could be distinguished in the ligament body (Fig. 7(a)).

The blood ligament narrowed with time and underwent several fragmentation phases. It occasionally ruptured firstly either at its lower end just near a primary drop or, more frequently, anywhere in the lower part of its body leaving a fragment attached to a primary drop (Fig. 7(b), (f) and (g)). It should be noted, however, that in several cases the initial blood ligament was observed to break first at the upper end or in the middle. The detached primary drop tended to merge with the adjacent ligament fragment while moving downward.

The ligament could subsequently break in one or more places along its length.

Finally, the ligament ruptured close the residual liquid (the liquid which remained attached to the object). The size of the ligament fragment remaining connected to the residual liquid after

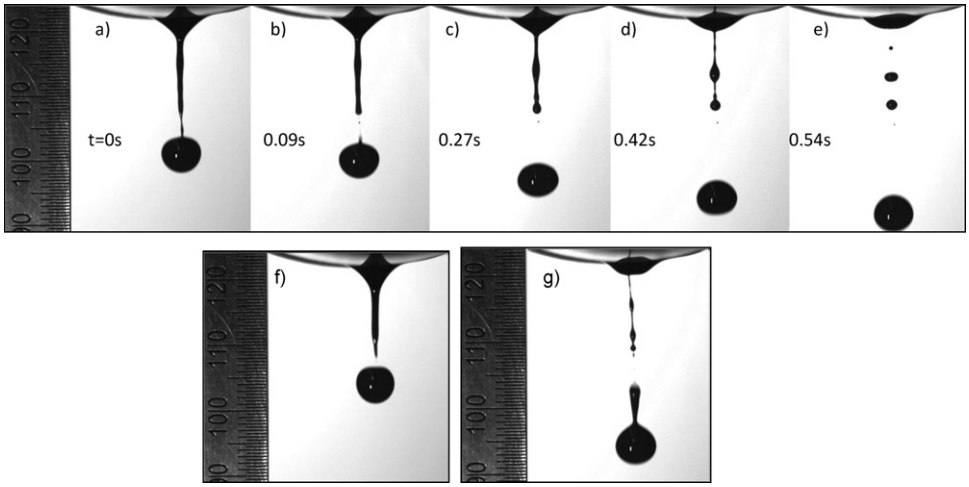

Fig. 7. Dripping of porcine blood from the cylindrical object with $H = 0.013\ mm^{-1}$ and 2.4 μm surface roughness. (b), (f) and (g) are observed variants of the primary drop detachment. The smallest scale division is 0.5 mm.

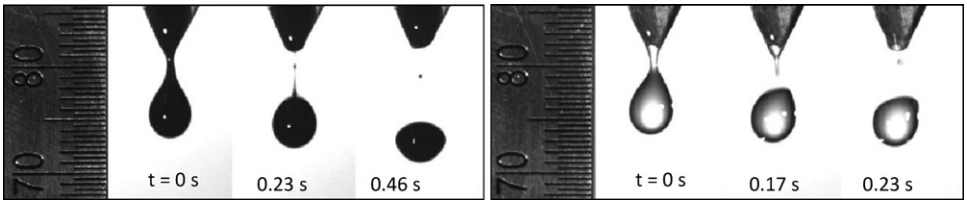

Fig. 8. Porcine blood and distilled water dripping from a knife tip. Smallest scale division is 0.5 mm.

the detachment varied from case to case. It was generally drawn back into the residual liquid.

Just prior to ligament breakup, thin threads were formed at the point of rupture which then produced one or more small droplets. Following this, the fragments of the ligament contracted into accompanying droplets (Fig. 7(c)–(e)). Occasionally, one drop was seen to bounce off another. This is a recognized phenomenon which occurs over a certain range of Weber numbers and impact parameter [36].

The fragmentation process seemed to differ for ligaments of different lengths. In particular, shorter ligaments, as seen during dripping from a knife, tended to rupture in only one or two places and subsequently produced fewer accompanying droplets (Fig. 8).

It was observed that longer ligaments were formed on larger objects, both for water and blood. However, blood ligaments tended to be longer than those of water.

Once separated from the ligament, primary blood and water drops continued to fall and experienced shape oscillations which damped with time. The amplitude of the oscillation seemed to depend on the way the drop was formed. The frequency of oscillation is known to depend on drop volume and surface tension and the rate of damping on viscosity [37]. In the present work blood drop oscillations were observed to damp more quickly than water drops.

4. Discussion

4.1. Effect of object size

The formation of larger primary drops from the less curved objects can be understood in terms of the increase in an available wetting area (Fig. 9). On an object of greater radius of curvature, the edges of the suspended mass lie at an angle closer to the horizontal (and the vertical component of the surface tension force is smaller), unless the suspended mass extends further around the object. The greater wetted area leads to an increase in total interfacial tension forces between the liquid and object surface which in turn can support a greater mass of liquid before it detaches. In addition, more liquid is available to flow into the ligament body as it extends, producing a large number of accompanying droplets. This effect, however, is not pronounced, possibly due to the low rate of liquid inflow.

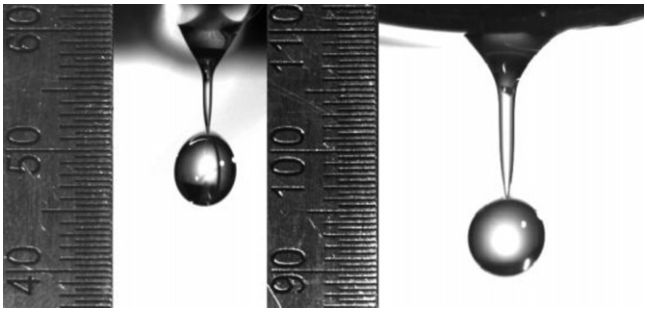

Fig. 9. Dripping of water from (a) the cylinder with $H = 0.1\ mm^{-1}$ and 0.66 μm surface roughness and (b) form the cylinder with $H = 0.01\ mm^{-1}$ and 0.19 μm surface roughness. The smallest scale division is 0.5 mm.

4.2. Effect of liquid properties

The higher surface tension of water is believed to be responsible for the larger primary water drops in comparison to blood (see for example [38]). The higher surface tension of water supports a greater mass of liquid before the droplet separates.

The variability in the number of accompanying drops may be explained by the viscosity of the liquid. In particular, the higher viscosity of blood, especially at the low shear rates which occur in the dripping process, slows the liquid as it flows axially along the ligament. In addition, viscous forces damp capillary waves, stabilizing the ligament. Because of this blood ligaments tend to be longer and more uniform in diameter at the time of breakup, compared to water ligaments which have lower viscosity. This consequently leads to the formation of a slightly greater number of accompanying droplets as a result of the breakup of the longer blood ligaments.

It may be hypothesized that, due to the high elongational stresses generated during the evolution of the ligament, the viscoelastic nature of blood properties becomes apparent. The observed shape of the blood ligament with a number of liquid bulges on it may be associated with this viscoelasticity [39]. Similar structures were observed during the detachment of drops of dilute aqueous solutions of high molecular weight polymers exhibiting viscoelastic (with elevated elongational viscosity) behavior by Wagner et al. [40]. Alternatively, these bulges may simply be capillary waves on the surface of the ligament.

The main drop size does not seem to be influenced by the fluid viscosity since the velocity gradients during the drip formation process are low. However, the variability in the observed main blood drop sizes may be related to the variability of the ligament fragmentation process. Notably, whether the ligament first breaks up near the end where it joins the primary drop, or closer to the object. The latter case implies an increase in the drop volume due to merging with the attached ligament fragment.

A study of the motion and breakup of ligaments of liquids with different viscosities by Handerson et al. [41] proposed a criterion for a ligament breakup/pinch off location based on the growth rate of disturbances with various wave numbers. In short, a ligament breaks up in one or more interior points if the wavelength of the most unstable wave mode is shorter then the ligament length. The breakup occurs at the ends when the wavelength is approximately equal to the ligament length.

The complexity of the blood ligament formation, elongation and fragmentation invites further investigation.

EDTA, used to prevent blood coagulation in this study, was observed previously to slightly increase blood density, viscosity and surface tension of blood. This might have caused a slight increase in the sizes of primary blood drops and formation of longer blood ligaments and, consequently, more satellite droplets.

The detailed study of the influence of different anticoagulants on physical properties of blood will be addressed in future publications of this research group.

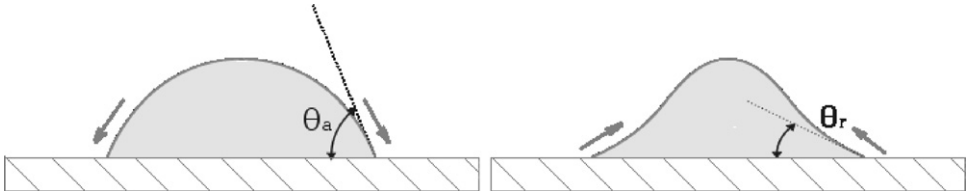

Fig. 10. Diagram of advancing θ_a and receding θ_r contact angles.

4.3. Effect of surface roughness

The surface roughness of the flat plates, with a cross-hatched surface texturing, appeared to have little effect on either primary drop size or number of accompanying drops. There was a weak dependence of primary water drop size on the roughness of the cylinders, and possibly a still weaker dependence when the fluid is blood.

The role of the unidirectional texturing of the machined objects, meaning a complex periodic surface structure of parallel peaks and valleys, in the drop formation process should be considered in relation to the wetting phenomenon. A static or equilibrium angle between the solid–liquid interface and the liquid–air interface at the point of contact, called the contact angle θ (Fig. 10), is used to quantitatively describe wetting and is defined by the Young–Dupre equation [42–44].

The static contact angle on a rough surface generically differs from the contact angle θ_0 on an ideal (flat, rigid, smooth and chemically homogeneous) surface. In addition there is contact-angle hysteresis on non-ideal surfaces, defined as the difference between the advancing θ_a and receding θ_r contact angles during the dynamic wetting (Fig. 10).

Liquid can wet a rough surface by filling in the troughs between the surface asperities [45].

Assuming that the surface roughness scale is insignificantly small compared to the dimensions of the liquid–solid contact area, the apparent contact angle is believed to depend on the ratio of actual to projected wetted area, called the roughness ratio, and increases with roughness if $\theta_0 > 90^\circ$. Whereas, for $\theta_0 < 90^\circ$ it decreases with roughness compared to the contact angle on the smooth surface [46].

This implies that hydrophobic surfaces become more hydrophobic, while hydrophilic surfaces become more hydrophilic when microtextructured. Consequently the liquid tends to spread more easily and cover larger areas on a rough hydrophilic surface.

The stainless steel used for the test objects has a high surface energy and exhibits hydrophilic properties where $\theta_0 < 90^\circ$, which indicates its high degree of wettability by water [47,48]. The observed contact angles on the flat plate samples tested were $\theta_0 < 90^\circ$.

From the present data, it is suggested that an increase in the area (and perimeter) covered by the liquid (caused by the decrease in contact angle) on roughening leads to an increase in the interfacial forces which in turn support larger liquid drops on rougher objects than on smoother objects.

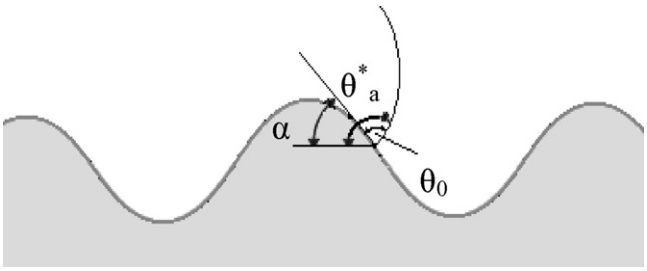

Fig. 11. The increase in advancing contact angle θ_a^* due to the slope of a surface asperity α.

In some cases (if the contact angle is large and the surface sufficiently rough), however, a thin layer of gas can be left between the liquid and solid surface [49,50]. Such a system must be largely hydrophobic with relatively high contact angles, and is unlikely in the present system.

Asperities on rough surfaces could pose significant barriers for a liquid flow especially if the roughness scale is relatively high [51–55]. This results in the pinning of a contact line and an increase in an advancing contact angle depending on the slope of the surface asperities/roughness at the liquid perimeter (α) for both roughened wetted and non-wetted surfaces (Fig. 11).

This effect may explain the formation of the smallest passive drops from the rough objects tested as a result of the reduction in the interfacial forces proportional to a decrease in the liquid–solid contact perimeter which accompanies a decrease in the contact angle on a sufficiently rough surface.

The combination of opposing effects (increasing surface roughness increases fluid contact area, but also exacerbates contact line pinning, perhaps limiting the fluid contact area) may explain the maximum in primary water drop size seen at medium roughness, with smaller drops occurring when the roughness is either increased or decreased. However there is not yet sufficient data to draw a firm conclusion. In any case, the size of the primary drops varies little with roughness value (R_a) suggesting only slight alteration of the available for wetting area (and perimeter) over the roughness range studied.

It should be noted that the influence of the surface texture on wetting is not limited to the effects of surface roughness (R_a) only, but the process may be influenced by other topological characteristics, for example, by the orientation and form of the roughness asperities [56].

The present results are for a flow rate of 0.1 mL/s only and the effect of varying flow rate would benefit from future study. Temperature and surface tension gradients, pressure fluctuations, air currents and evaporation may also affect drop formation mechanism, possibly inducing variability in resulting drop sizes, but this is expected to be small in the present study.

5. Conclusions

The process of passive dripping from (blunt and sharp) objects with different surface curvatures and roughnesses has been studied with high speed video and the size of the primary drops and number of accompanying drops have been measured. These objects were chosen to represent weapons that might be used during the commission of a crime. Distilled water and porcine blood, controlled so that the surface tension and viscosity fell within the normal human range, were used.

Previous observations [6,8,9] that the size of a primary passive blood drop decreases as the surface curvature of the object from which it drips increases, have been confirmed by our findings, and systematically quantified. Blood drop volumes of between 37.4 μL (knife) and 121.8 μL (cylinder with $H = 0.01\ \text{mm}^{-1}$ and 3.59 μm roughness) were recorded. The primary drop size was, however,

relatively insensitive to the size of the object if the mean curvature of its surface was smaller than 0.10 mm^{-1} (primary blood drop size 87–125 μL, diameter 5.5–6.2 mm in this range). Surface roughness influenced drop size only weakly for the cylinders studied, and not at all for flat plates, so surface roughness not a complicating factor, over the hydrophobicity and the range of roughnesses studied.

Blood on average tended to produce a slightly greater number of accompanying droplets than water and there was some dependence on object size, but the number of accompanying droplets showed great variability even under nominally identical conditions. The surface roughness had a small effect on the drop formation mechanism, over the roughness range studied.

It is possible, under favorable conditions, to infer the impact velocity and hence fall height of a passive drop hitting a target surface, from the stain size, if the primary drop volume can be ascertained using a correlation such as that between stain spreading and the impact Weber number [13]. We speculate that primary drop size could be estimated for smaller weapons if the shape and surface roughness of the dripping object is known. It may also be possible to distinguish dripping from blunt objects such as baseball bats and iron bars from that of sharp weapons such as knives and screwdrivers. However further work is required to determine the reliability of such methods when factors such as temperature, movement or vibration of the object and blood composition are considered.

Acknowledgments

We would like to thank Romain Vermorel, Antonin Puybareau, Clement Christmann, and Eric Texier for their work on early versions of the experimental apparatus. We thank Bart Epstein and Terry Laber of the Minnesota Bureau of Criminal Apprehension for their generous advice and inspiration. The technical staff of the Mechanical Engineering Workshop and Laboratories contributed essential work, advice and encouragement throughout. N.K. was funded by a University of Canterbury Doctoral Scholarship, and E.W. by ESR Scholarships.

References

[1] T.L. Laber, Diameter of a bloodstain as a function of origin, distance fallen, and volume of a drop, IABPA News 2 (1) (1985) 12–16.
[2] P.A. Pizzola, S. Roth, P.R. De Forest, Blood droplet dynamics-I, J. Forensic Sci. 31 (1) (1986) 36–49.
[3] N. Rogers, Hematocrit – Implications for Bloodstain Pattern Analysis, Centre for Forensic Science, University of Western Australia, Perth, 2009, p. 128.
[4] N.L. Parker, L.R. Bedore, K.K. Cooper, P. Fowler, T.A. Miller, J. Showalter, Summary Report of Bloodstain Pattern Analysis Research Group, 1982, pp. 1–91.
[5] E.S. Ross, The study of bloodstain patterns resulting from the release of blood drops from a weapon, in: Chemistry, The University of Auckland, Auckland, 2006
[6] V. Balthazard, R. Piedlievre, H. Desoille, L. DeRobert, Etude des gouttes de sang projete (study of projected drops of blood), in: Annual Medecine Legale Criminol Police Science Toxicology, 22nd Congress of Forensic Medicine, Paris, France, (1939), pp. 265–323.
[7] H.L. MacDonell, K. DeLije, On measuring the volume of very small drops of blood and correlation of this relationship to bloodstain diameter, in: 5th Meeting of the International Association of Bloodstain Pattern Analysts, Dallas, TX, 1989.
[8] C. Knock, M. Davison, Predicting the position of the source of blood stains for angled impacts, J. Forensic Sci. 52 (5) (2007) 1044–1049.
[9] L. Hulse-Smith, N.Z. Mehdizadeh, S. Chandra, Deducing drop size and impact velocity from circular bloodstains, J. Forensic Sci. 50 (1) (2005) 1–10.
[10] L. Hulse-Smith, M. Illes, A blind trial evaluation of a crime scene methodology for deducting impact velocity and droplet size from circular bloodstains, J. Forensic Sci. 52 (1) (2007) 65–69.
[11] S. Fordham, On the calculation of surface tension from measurements of pendant drops, Proc. R. Soc. Lond. A 194 (1036) (1948) 1–16.
[12] C.E. Stauffer, The measurement of surface tension by the pendant drop technique, J. Phys. Chem. 69 (6) (1965) 1933–1938.
[13] Y. Tanasawa, S. Toyoda, Technical Report of Tohoku University, Japan, N19-2, 1955, p. 135.
[14] D.T. Papageorgiou, On the breakup of viscous liquid threads, Phys. Fluids 7 (1995) 1529–1544.
[15] J. Eggers, Universal pinching of 3D axisymmetric free-surface flow, Phys. Rev. Lett. 71 (1993) p.3458–p.3460.
[16] A.Y. Tong, Z. Wang, Relaxation dynamics of a free elongated liquid ligament, Phys. Fluids 19 (2007), 092101-1-11.
[17] P. Maromottant, E. Willermaux, Fragmentation of stretched liquid ligaments, Phys. Fluids 16 (2004) 2732–2742.
[18] C. Pozrikidis, Stability of sessile and pendant drops, J. Eng. Math. 72 (2012) 1–20.
[19] A.H. Lefebvre, Atomization and Sprays, Hemisphere, New York, 1989.
[20] C.E. Lapple, J.P. Henry, D.E. Blake, Atomization – A Survey and Critique of the Literature, Stanford Research Institute Technical Report, 1957, N6.
[21] K. Tamada, Y. Shibaoka, On the pendent drop, Int. J. Phy. Soc. Jpn. 16 (6) (1961) 1249–1252.
[22] K. Hida, T. Nakanishi, The shape of a bubble or a drop attached to a flate plate, J. Phys. Soc. Jpn. 28 (5) (1970) 1336–1339.
[23] M.A. Raymond, E.R. Smith, J. Liesegang, The physical properties of blood – forensic considerations, Sci. Justice 36 (3) (1996) 153–160.
[24] J.V. Dacie, S.M. Lewis, Practical Haemotology, Churchill Livingstone, London, 1995 , pp. 12–17.
[25] R.J. Trudnowski, R.C. Rico, Specific gravity of blood and plasma at 4 and 37 °C, Clin. Chem. 20 (5) (1974) 615–616.
[26] H. Hinghofer-Szalkay, J.E. Greenleaf, Continuous monitoring of blood volume changes in humans, J. Appl. Physiol. 63 (3) (1987) 1003–1007.
[27] T. Kenner, The measurement of blood density and its meaning, Basic Res. Cardiol. 184 (1989) 111–124.
[28] E. Hrncir, J. Rosina, Surface tension of blood, Physiol. Res. 46 (4) (1997) 319–321.
[29] J. Rosina, E. Kvašňák, D. Šuta, H. Kolářová, J. Málek, L. Krajči, Temperature dependence of blood surface tension, Physiol. Res. 56 (Suppl. 1) (2007) S93–S98.
[30] G.D.O. Lowe, J.C. Barbenel, Plasma and blood viscosity, in: G.D.O. Lowe (Ed.), Clinical Blood Rheology, Vol. 1, CRC Press, Boca Ration, FL, 1988, pp. 11–44.
[31] R.E. Wells, R. Denton, E.W. Merrill, Measurement of viscosity of biologic fluids by cone plate viscometer, J. Lab. Clin. Med. 57 (4) (1961) 646–656.
[32] S. Casson, G. Kurland, Viscometry of human blood for shear rates of 0–100,000 s^{-1}, Nature 206 (1965) 617–618.
[33] S. Chien, Determinants of blood viscosity and red cell deformability, J. Clin. Lab. Investig. 156 (1981) 7–12.
[34] E. Ernst, Ch. Monshausen, A. Matrai, Blood viscosity – a comparative study on three rotational instruments, Biorheology 22 (1985) 471–475.
[35] W.M. Haynes (Ed.), CRC Handbook of Chemistry and Physics, 92nd ed., CRC Press/Taylor and Francis, Boca Raton, FL, 2012.
[36] J. Qian, C.K. Law, Regimes of coalescence and separation in drop collision, J. Fluid Mech. 33 (1997) 59–80.
[37] M.A. Raymond, E.R. Smith, J. Liesegang, Oscillating blood droplets—implications for crime scene reconstruction, Sci. Justice 36 (1996) 161–171.
[38] X. Zhang, O.A. Basaran, An experimental study of dynamics of drop formation, Phys. Fluids 7 (1995) 1184.
[39] G. Thurston, Viscoelasticity of human blood, Biophys. J. 12 (1972) 1205–1217.
[40] C. Wagner, Y. Amarouchene, D. Bonn, J. Eggers, Droplet detachment and satellite bead formation in viscoelastic fluids, Phys. Rev. Lett. 95 (2005) 1645041–1645044.
[41] D. Hunderson, H. Segur, L. Smolka, M. Wadati, The motion of a falling liquid filament, Phys. Fluids 12 (3) (2000) 550–563.
[42] (a) T. Young, An essay on the cohesion of fluids, Phil. Trans. R. Soc. Lond. 95 (1805) 65–87;
(b) See also T. Young, in: G. Peacock (Ed.), Miscellaneous Works, vol. 1, Murray, London, 1855, p. 418.
[43] A. Dupré, Theorie Mecanique de la Chaleur, Gauthier-Villars, Paris, 1869, p. 368.
[44] A.W. Adamson, Physical Chemistry of Surfaces, 5th ed., Wiley-Interscience Publication, New York, 1990.
[45] R.N. Wenzel, Resistance of solid surface to wetting by water, Ind. Eng. Chem. 28 (1936) 988–994.
[46] (a) R.J. Good, A thermodynamic derivation of Wenzel's modification of Young's equation for contact angles; together with a Theory of Hysteresis, J. Am. Chem. Soc. 74 (1952) 5041;
(b) See also R.J. Good, Contact angle, wetting, and adhesion: a critical review, J. Adhes. Sci. Technol. 6 (12) (1992) 1269–1302.
[47] N. Thongyai, Study of stainless steel surface cleanability, MS Thesis, King Mongkut's Institute of Technology, North Bangkok, 2005.
[48] H.S. Kim, W.S. Kang, S.H. Hong, Metal surface treatment for enhancement of hydrophilic property using atmospheric-pressure dielectric barrier discharge, IEEE Transl. Plasma Sci. 38 (2010) 1982.
[49] A.B.D. Cassie, S. Baxter, Wettability of porous surfaces, Trans. Faraday Soc. 40 (1944) 546–551.
[50] A.B.D. Cassie, Contact angles, Discuss. Faraday Soc. 3 (1948) 11–16.
[51] R. Shuttleworth, G.L.J. Bailey, The spreading of a liquid over a rough solid, Discuss. Faraday Soc. 3 (1948) 16–22.
[52] R.E. Johnson, R.H. Dettre, Wetting and contact angle, Surf. Colloid Sci. 2 (1969) 85–153.
[53] C. Huh, S.G. Mason, Effects of surface roughness on wetting (theoretical), J. Colloid Interface Sci. 60 (1977) 11–38.
[54] J.D. Eick, R.J. Good, A.W. Neumann, Thermodynamics of contact angles. II. Rough solid surfaces, J. Colloid Interface Sci. 53 (1975) 235–238.
[55] S.J. Hitchcock, N.T. Carrol, M.G. Nicholas, Some effects of substrate roughness on wettability, J. Mater. Sci. 16 (1981) 714–732.
[56] A.W. Neumann, R.J. Good, Techniques of measuring contact angles, Surf. Colloid Sci. 11 (1979) 31–91.